Mie theory, Airy theory, and the natural rainbow

Raymond L. Lee, Jr.

Compared with Mie scattering theory, Airy rainbow theory clearly miscalculates some monochromatic details of scattering by small water drops. Yet when monodisperse Airy theory is measured by perceptual (rather than purely physical) standards such as chromaticity and luminance contrast, it differs very little from Mie theory. Considering only the angular positions of luminance extrema, Airy theory's errors are largest for small droplets such as those that dominate cloudbows and fogbows. However, integrating over a realistic drop-size distribution for these bows eliminates most perceptible color and luminance differences between the two theories. © 1998 Optical Society of America

OCIS codes: 010.1290, 290.4020, 090.5640, 260.5430.

1. Introduction

A commonplace of optics history is that Newton's (and Descartes') geometrical optics dominated 18th-century rainbow theory. Similarly, George Airy's 1838 interference/diffraction theory[1] built on Thomas Young's work and held sway for several decades in the 19th century, although not without early detractors. The ascendance of these theories depended on their ability to explain naked-eye features of the natural rainbow (i.e., bows seen in rain, clouds, fog, or spray). However, Airy theory was soon held to a different standard: predicting the angular positions of intensity maxima and minima for spheres and cylinders illuminated by nearly monochromatic light.[2] Despite early success with such predictions, Airy theory was found wanting by 1888, when one experimenter said that his measurements showed it to be "but a first approximation."[3]

Today Airy theory is seldom compared with exacting measurements,[4] but rather with the intensity distribution functions of Mie theory.[5] Here Airy theory may not position the rainbow intensity extrema correctly, sometimes turning monochromatic maxima into minima and vice versa.[6,7] These discrepancies are most noticeable for small drop sizes and parallel-polarized rainbow light.[8] The limitations of Airy's cubic wave-front approximation prompted van de Hulst to conclude in 1957 that the "validity of Airy's theory is thus limited to [size parameters] $x > 5000$, or with light of $\lambda/2\pi = 0.1\ \mu$ to drops with radii $>½$ mm."[9] Naturally van de Hulst did not have the luxury of today's computer resources, so checking his analytic claim numerically would have been difficult. Yet, even in 1979, Mobbs cited van de Hulst's claim as one reason for developing his own rainbow theory.[10]

That same year, however, Können and de Boer extended Airy theory to include rainbow polarization and found that their visible-wavelength results were reliable at drop radii as small as ~0.14 mm.[11] Furthermore, in 1977 Nussenzveig described monochromatic modeling in which Airy's dominant $\perp$-polarized component "requires only small corrections within the primary bow, and its errors become appreciable only in the region of the supernumerary arcs." Still, he correctly noted that "Airy's approximation fails badly" for the $\|$-polarized primary.[12] In fairness, Wang and van de Hulst have recently qualified the earlier proscription: "We found that, *contrary to what has often been thought*, . . . , Airy theory starts to be useful at relatively small sizes. For a drop size of 0.1 mm it already represents the main maxima of the primary . . . and secondary . . . rainbows quite well" (emphasis added).[13]

The italics suggest an entrenched conventional wisdom. Certainly the implications of van de Hulst's and Nussenzveig's influential earlier analyses are clear: (1) Airy theory is of limited use in analyzing the rainbow, and (2) Mie theory (or at least a theory more sophisticated than Airy's) is necessary for quantitatively reliable rainbow studies. Können, de Boer, Sassen, Wang, and van de Hulst have partially exonerated Airy theory, but a whiff of the unsavory remains. Thus some fresh questions about rainbow verisimilitude are worth asking.

The author is with the Department of Oceanography, U.S. Naval Academy, Annapolis, Maryland 21402.

Received 14 May 1997; revised manuscript received 12 September 1997.
0003-6935/98/091506-14$15.00/0
© 1998 Optical Society of America

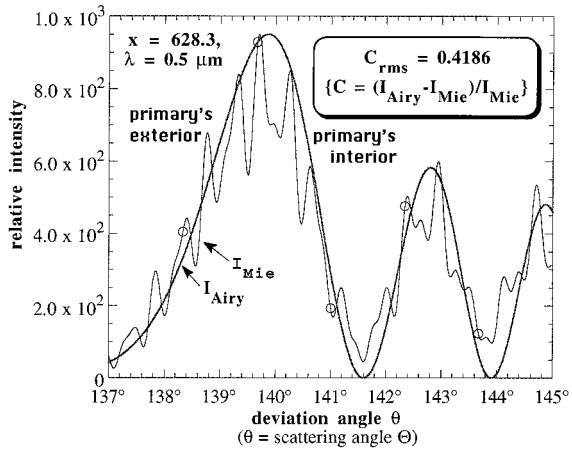

Fig. 1. Comparison of Mie and Airy intensity distribution functions at size parameter $x = 628.3$ for wavelength $\lambda = 0.5\ \mu$m and a drop radius of $r = 50\ \mu$m. In Figs. 1 and 2, $C_{\rm rms}$ is the root-mean-square distance between the two theories' intensities averaged over deviation angle $\theta = 137°–145°$.

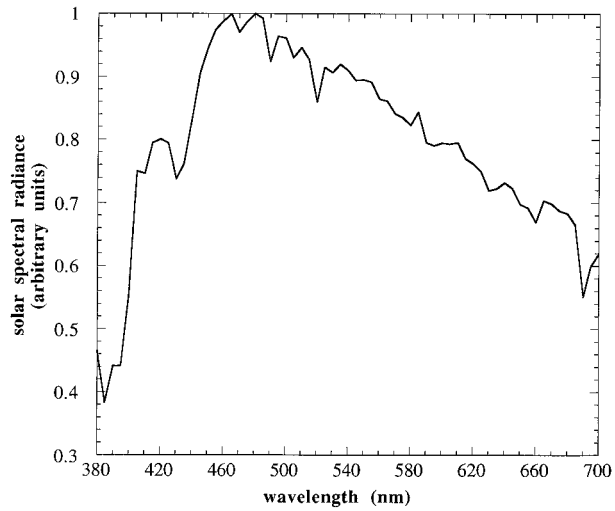

Fig. 3. Relative solar spectral radiance at a Sun elevation of ~45°, derived from measurements at University Park, Pa., on 5 October 1987. This is the spectral illuminant assumed in calculating Figs. 4–25 and 27–30, and its CIE 1976 uniform chromaticity scale coordinates are $u' = 0.1986$ and $v' = 0.4713$.

First, do the monochromatic shortcomings of Airy theory make it suspect in modeling what the naked-eye observer sees in the natural rainbow? In other words, should Airy theory be our rainbow theory of last resort? Second, how perceptible are Airy theory's photometric and colorimetric departures from Mie theory?

2. Setting the Theoretical Stage

Even a cursory comparison of Mie and Airy theories reveals distinct differences between their intensity distribution functions at a given wavelength and drop size. Figure 1 shows this difference in primary rainbows at wavelength $\lambda = 0.5\ \mu$m for water drops with radii $r = 50\ \mu$m ($x = 2\pi r/\lambda = 628.3$). Before beginning our comparison, however, we first must consider some issues of terminology and scaling. Figure 1's abscissa poses the first problem—Airy theory is usually couched in terms of deviation angle θ, whereas Mie theory uses scattering angle Θ. In primary bows, θ and Θ are the same, but in the secondaries $\Theta = 360° - \theta$. For consistency, I use deviation angle throughout this paper, mindful that Mie theory does not invoke deviated light rays.

The ordinate in Fig. 1 also requires the merging of two different systems, this time radiometric. To calculate Airy theory's intensities, I use the formulas of Humphreys,[14] Tricker,[15] and Können and de Boer.[16] Mie theory intensities are based on an algorithm by Bohren and Huffman and include the effects of external reflections.[17] For a given λ, r, and range of θ, the two theories can yield quite different intensity maxima, so I must normalize one theory's results in order to compare them with the other's. Here I scale

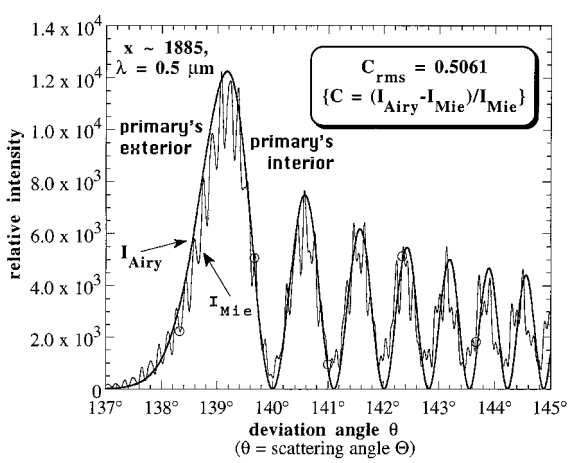

Fig. 2. Comparison of Mie and Airy intensity distribution functions at $x \sim 1885$ for $\lambda = 0.5\ \mu$m and $r = 150\ \mu$m.

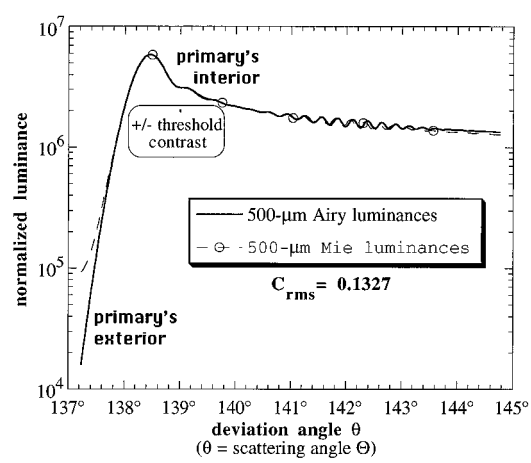

Fig. 4. Normalized Mie and Airy theory primary luminances as functions of deviation angle θ for a single 500-μm-radius raindrop (both polarizations). The two theories' intensity distribution functions are convolved with Fig. 3's illuminant to produce spectrally integrated luminances. These luminances are plotted in arbitrary units that are also used in Figs. 5–7 and 18–21.

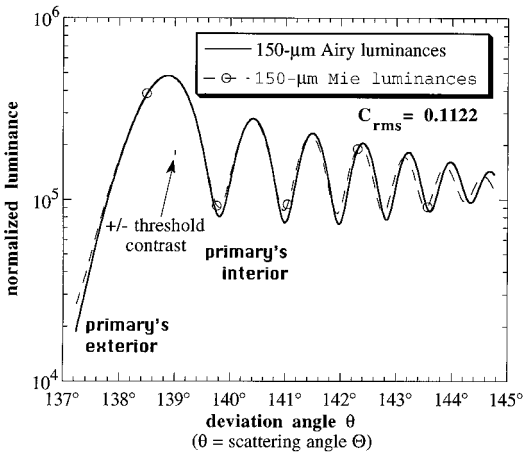

Fig. 5. Normalized Mie and Airy theory primary luminances as functions of deviation angle θ for a single 150-μm-radius drizzle drop (both polarizations).

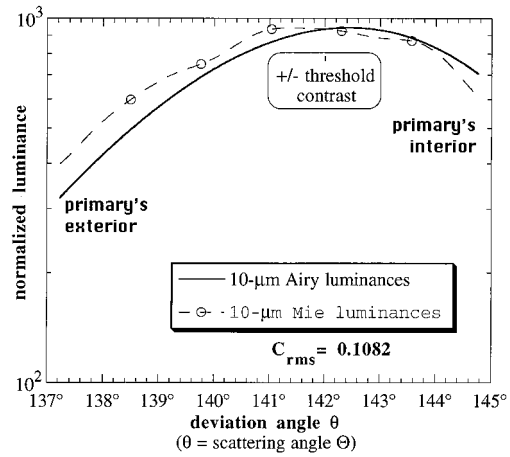

Fig. 7. Normalized Mie and Airy theory primary luminances as a function of deviation angle θ for a single 10-μm-radius cloud drop (both polarizations).

Airy theory curves by the normalizing factor $I_{max,Mie}/I_{max,Airy}$, where $I_{max,Mie}$ and $I_{max,Airy}$ are the respective intensity (or luminance L_v) maxima for the two Mie and Airy theory curves being compared. Thus in every figure that compares intensity (or luminance), my Airy and Mie maxima are the same. Other normalizations are possible, but they do not alter my qualitative conclusions.

In Fig. 1, the Mie ripple structure (both polarizations) is evident as it oscillates around the smoother Airy intensity curve (⊥ polarization only). Such monochromatic comparisons usually illustrate the failings of Airy theory, especially of its ‖-polarized component.[18] However, Fig. 1 also shows how the Airy ⊥-polarized component approximately follows the Mie extrema. At each θ and corresponding Θ in Fig. 1, I quantify this difference as an Airy–Mie contrast C, where $C = (I_{Airy} - I_{Mie})/I_{Mie}$. In Fig. 1, the root-mean-square (rms) contrast difference between the two theories is 0.4186. Contrary to expectations, this rms difference rises to 0.5061 for Fig. 2's larger drop radius (150 μm), an increase attributable both to larger excursions in the Mie ripple structure[19] and smaller Airy minima. Cast in these monochromatic terms, Airy theory is indeed a poor second to Mie theory.

However, if we compare the two theories' colors and luminances, the differences are subtler. My comparisons make some assumptions that are conservative (i.e., they preserve some Mie scattering details) and sometimes literally unnatural (i.e., they do not include all factors affecting natural bows). Thus I am not relentlessly smoothing away Mie theory details, but instead examining whether they result in

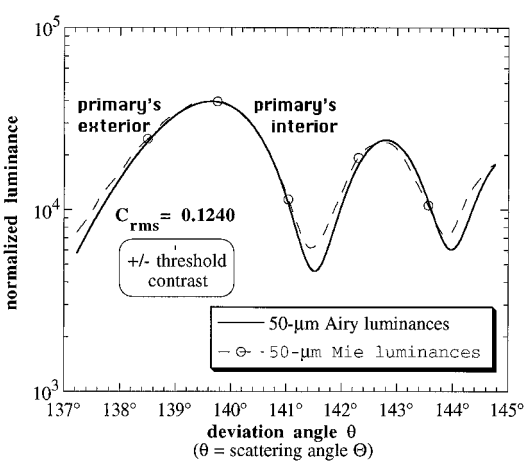

Fig. 6. Normalized Mie and Airy theory primary luminances as functions of deviation angle θ for a single 50-μm-radius cloud drop (both polarizations).

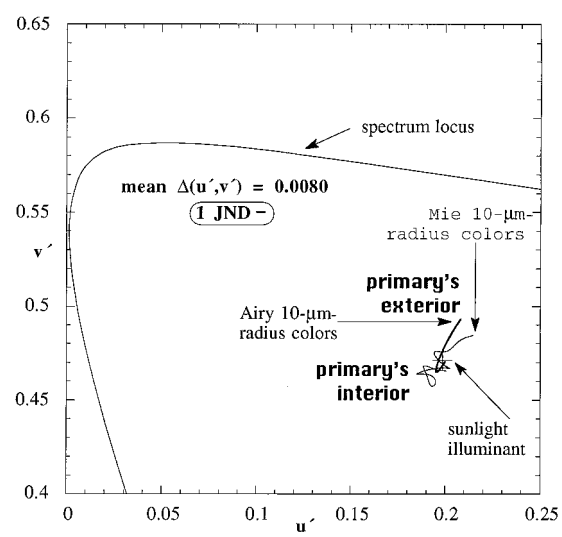

Fig. 8. Portion of the CIE 1976 UCS diagram, showing the chromaticity of Fig. 3's illuminant (+) and separate $u'(\theta)$, $v'(\theta)$ chromaticity curves for Airy and Mie theory primary cloudbows at 10-μm radius (both polarizations). The two curves' mean colorimetric separation $\overline{\Delta(u', v')} = 0.0080$, compared with a mean MacAdam JND of 0.004478 in the u', v' region spanned by the Mie and the Airy primaries.

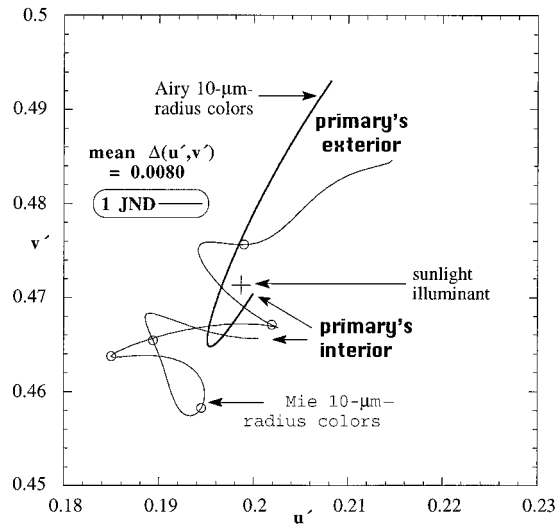

Fig. 9. Close-up view of Fig. 8. Note that the u', v' scaling is isotropic in this and all subsequent UCS diagrams.

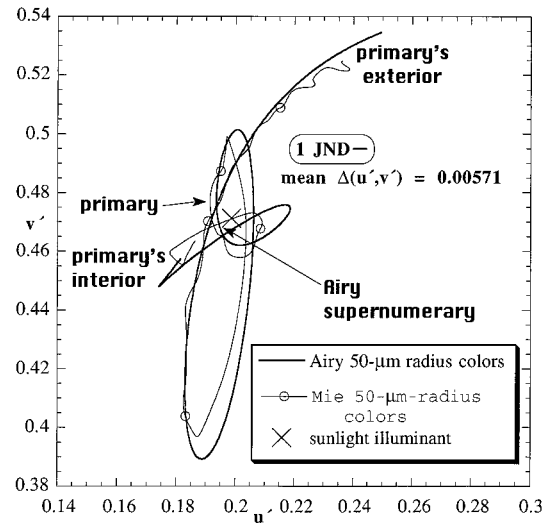

Fig. 11. Chromaticity curves for the 50-μm-radius Airy and Mie theory primaries differ by $\overline{\Delta(u', v')} = 0.00571$ (both polarizations).

rainbow features visible to naked-eye observers. In all that follows, bear in mind that I am not emphasizing the two theories' electromagnetic or mathematical details, but instead their visible differences.

First, unlike Figs. 1 and 2, all subsequent figures describe the convolution of a rainbow intensity distribution function and a particular illuminant. Figure 3 shows this illuminant's spectrum, which corresponds to sunlight measured at the Earth's surface when the Sun's elevation is ~45°. Obviously very few rainbows will be seen for a 45° Sun elevation,[20] but my point here is simply to choose a natural illuminant that is not highly chromatic. Second, all subsequent figures include the smoothing effects of sunlight's approximately 0.5° angular divergence.[21] Third, all comparisons include both the ⊥- and the ∥-polarized components of rainbow light, just as the naked-eye observer must. However, except in two cases, I do make the unnatural assumption that only a single, spherical drop generates the bows. In other words, because I integrate over a drop-size distribution only rarely, my canonical comparison is between monodisperse luminances and chromaticities for Mie and Airy theories.

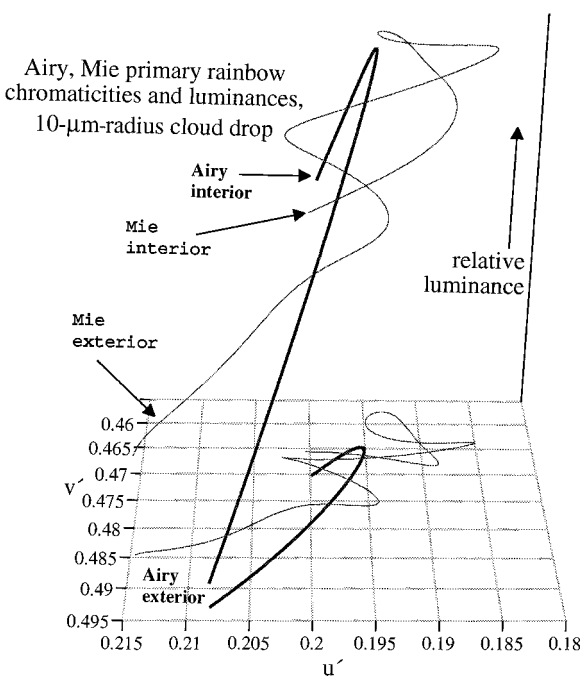

Fig. 10. Perspective view that combines chromaticities (Fig. 9) and luminances (Fig. 7) for Mie and Airy theory 10-μm-radius primary cloudbows (both polarizations). The combined luminance and chromaticity curves are also shown projected on the u', v' chromaticity plane.

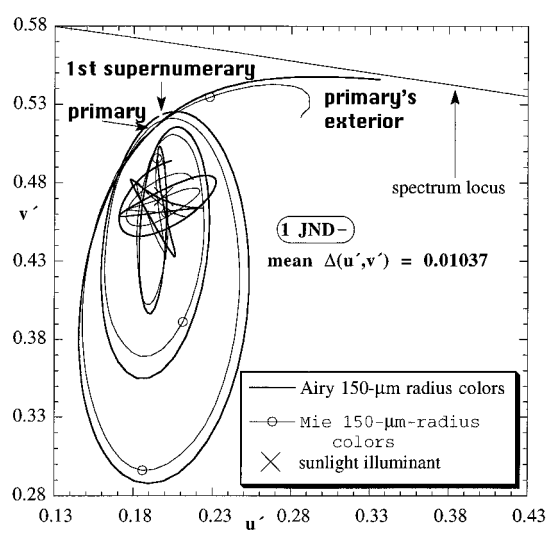

Fig. 12. Chromaticity curves for the 150-μm-radius Airy and Mie theory primaries differ by $\overline{\Delta(u', v')} = 0.01037$ (both polarizations). Breaks in the Airy curve mark the positions of its primary and first supernumerary.

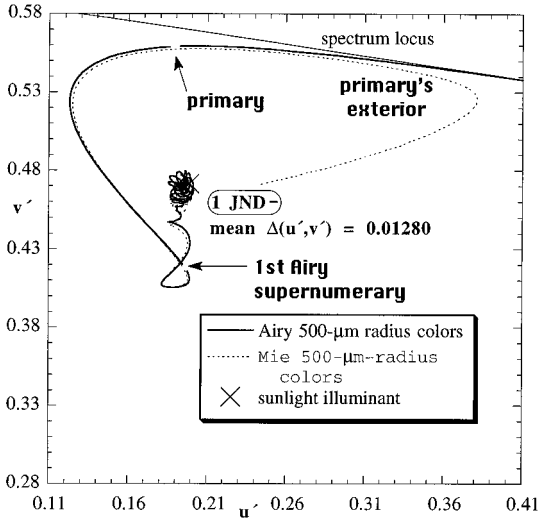

Fig. 13. Chromaticity curves for the 500-μm-radius Airy and Mie theory primaries differ by $\overline{\Delta(u', v')} = 0.01280$ (both polarizations).

3. Monodisperse Comparisons of Mie and Airy Primaries

We begin by comparing the spectrally integrated relative luminances $L_v(\theta)$ of single-droplet primary rainbows and cloudbows with drop radii of 500, 150, 50, and 10 μm.[22] For a large 500-μm-radius drop, Fig. 4 shows the expected close agreement between Airy and Mie theories.[23] Now define luminance contrast as $C_v = [(L_{v,\mathrm{Airy}} - L_{v,\mathrm{Mie}})/L_{v,\mathrm{Mie}}]$. At a given drop radius, C_v is averaged over N discrete $L_v(\theta_i)$ to yield the rms contrast C_{rms}, where

$$C_{\mathrm{rms}} = \left\{ \sum_{i=1}^{N} \left[\frac{L_{v,\mathrm{Airy}}(\theta_i) - L_{v,\mathrm{Mie}}(\theta_i)}{L_{v,\mathrm{Mie}}(\theta_i)} \right]^2 / N \right\}^{1/2} \tag{1}$$

and $N = 383$. In Fig. 4, $C_{\mathrm{rms}} = 0.1327$, a much smaller value than those for the monochromatic Figs. 1 and 2. Not surprisingly, integration over the visible spectrum eliminates much of the Airy–Mie luminance difference. Like most contrast measures, C_v scales luminance differences in terms of some reference luminance, which here is $L_{v,\mathrm{Mie}}$. Thus C_{rms} shows relative departures from our Mie rainbow standard, and those departures are averaged across the deviation angle.

Note that integration over the Sun's diameter in Fig. 4 reduces the original $L_v(\theta)$ to the range $137.23° \leq \theta \leq 144.76°$. This integration takes the form

$$L_S(\theta) = \int_{\theta-w}^{\theta+w} \left[1 - \left(\frac{\theta - \vartheta}{w} \right)^2 \right]^{1/2} L_v(\vartheta) \mathrm{d}\vartheta, \tag{2}$$

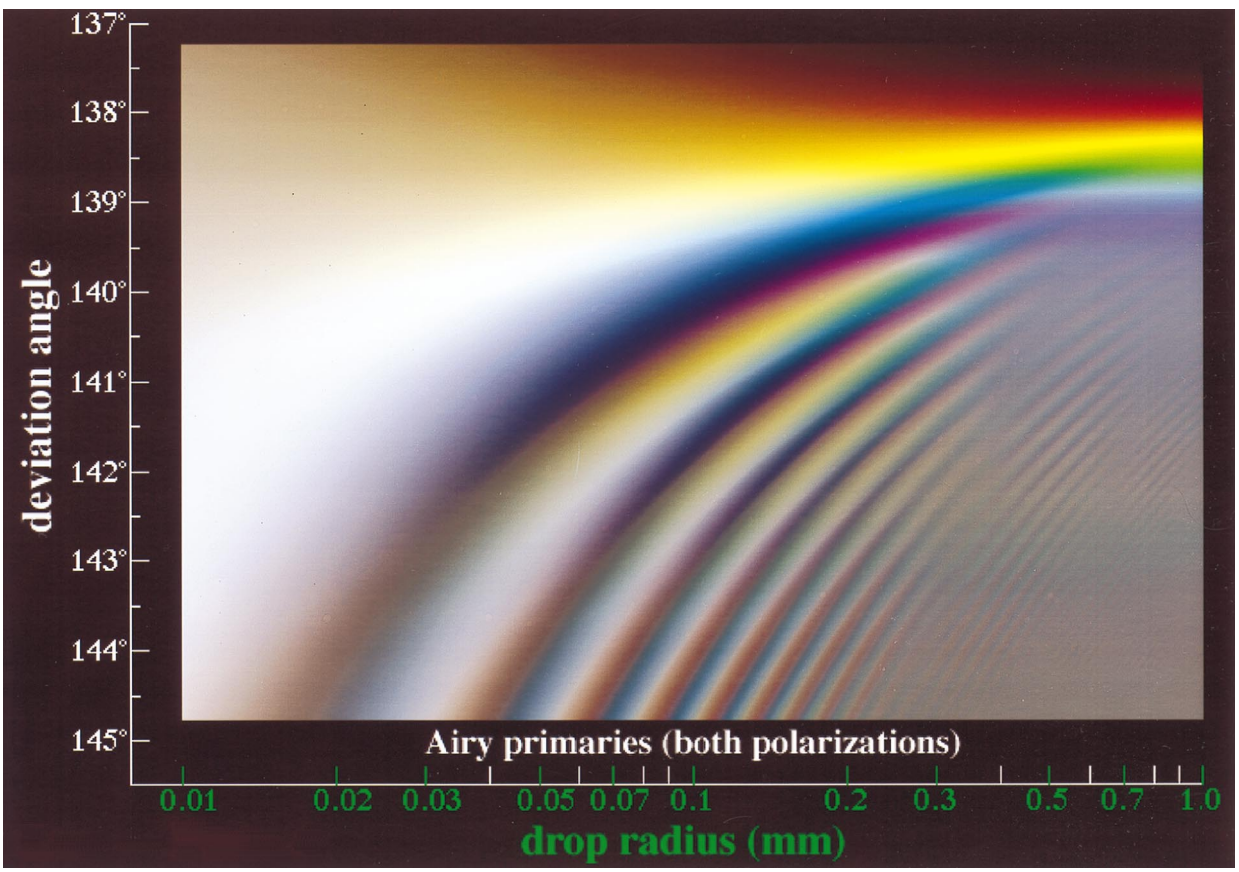

Fig. 14. Map of Airy theory colors for monodisperse primary rainbows and cloudbows. The map assumes (1) Fig. 3's solar spectrum as the illuminant, (2) Eq. (2)'s sun-width smoothing filter, (3) both rainbow polarizations, (4) spherical, nonabsorbing water drops. At each drop radius, colors' luminances are normalized by the maximum luminance for that radius. A colorimetrically calibrated version of this figure can be seen at the www address given in the acknowledgment.

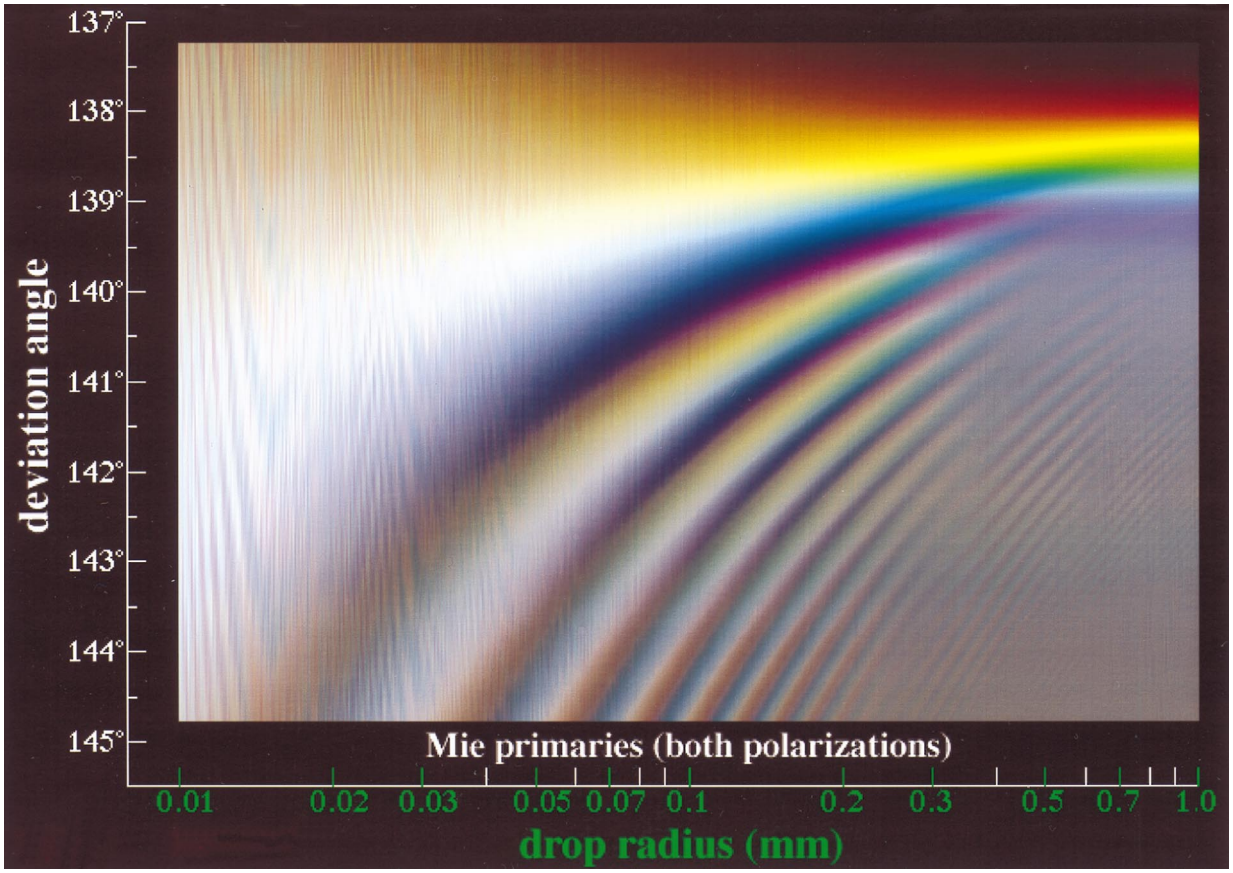

Fig. 15. Map of Mie theory colors for monodisperse primary rainbows and cloudbows. Figure 14's assumptions (1)–(4) also hold here. A colorimetrically calibrated version of this figure can be seen at the www address given in the acknowledgment.

where $L_S(\theta)$ is the smoothed luminance and w is the solar radius of ~0.25° [all Eq. (2) angles are in radians]. Equation (2)'s square-root term is proportional to the Sun's angular width at each radial angle ϑ across the Sun's disk. In effect, at each θ we approximate the finite-width sun as the sum of many point-source suns, each of which is weighted by the real Sun's angular width at radial angle ϑ. In turn, each point-source sun contributes its own rainbow $L_v(\vartheta)$ to the observed $L_S(\theta)$. Integrals similar to Eq. (2) smooth the Mie and the Airy chromaticities discussed below.

How significant visually are Fig. 4's C_{rms}? Small tick marks shown in the ± threshold contrast boxes of Figs. 4–7 provide one indication. Each tick mark spans a luminance range that is ±2% of its mean value. If a ±2% luminance change is a just-noticeable difference[24] (JND), then Fig. 4's tick mark is a graphical measure of threshold contrast. Note that Fig. 4's tick mark will have the same length anywhere along its logarithmic ordinate, although that length will change when the ordinate's range changes. Gauged in terms of contrast, then, most Airy–Mie luminance differences in Fig. 4 are subthreshold (i.e., they are invisible). Even in the supernumeraries (θ = 141°–143.5°), Fig. 4's Airy theory errors usually are invisible. The largest disagreement occurs in Alexander's dark band ($\theta < 137.6°$), where Mie theory consistently predicts more light.[25] Yet the overall close agreement in Fig. 4 is not surprising, because the mean visible-wavelength size parameter $\bar{x} = 6004$ here, which exceeds van de Hulst's 1957 lower limit on Airy theory's validity.

Figure 5 shows Airy and Mie luminances for a 150-μm drizzle drop. C_{rms} has decreased slightly to 0.1122, as has the luminance difference in Alexander's dark band. However, the Airy underestimates of luminance in the supernumerary minima now are near or above threshold. Supernumerary maxima are still indistinguishably different in the two theories. Although $\bar{x}$ (150 μm) = 1801, Airy departures from Mie theory still are not pervasive. However, in Fig. 6's 50-μm cloudbow ($\bar{x} = 600$), small angular offsets of the Airy supernumeraries from their Mie counterparts are now evident even in the first supernumerary. Airy supernumerary minima are now noticeably darker than those for Mie theory, as the increase of C_{rms} to 0.1240 suggests.

For a small cloud drop (10-μm radius, $\bar{x} = 120$), the two bows have broadened sufficiently in Fig. 7 that no supernumeraries are visible, although residual ripple-structure fluctuations are still evident in the Mie cloudbow. (These luminance ripples do have a color counterpart, as shown below.) Although C_{rms} is smaller (0.1082) than that for Fig. 6's larger cloud drop, Fig. 7's Mie and Airy curves are even less con-

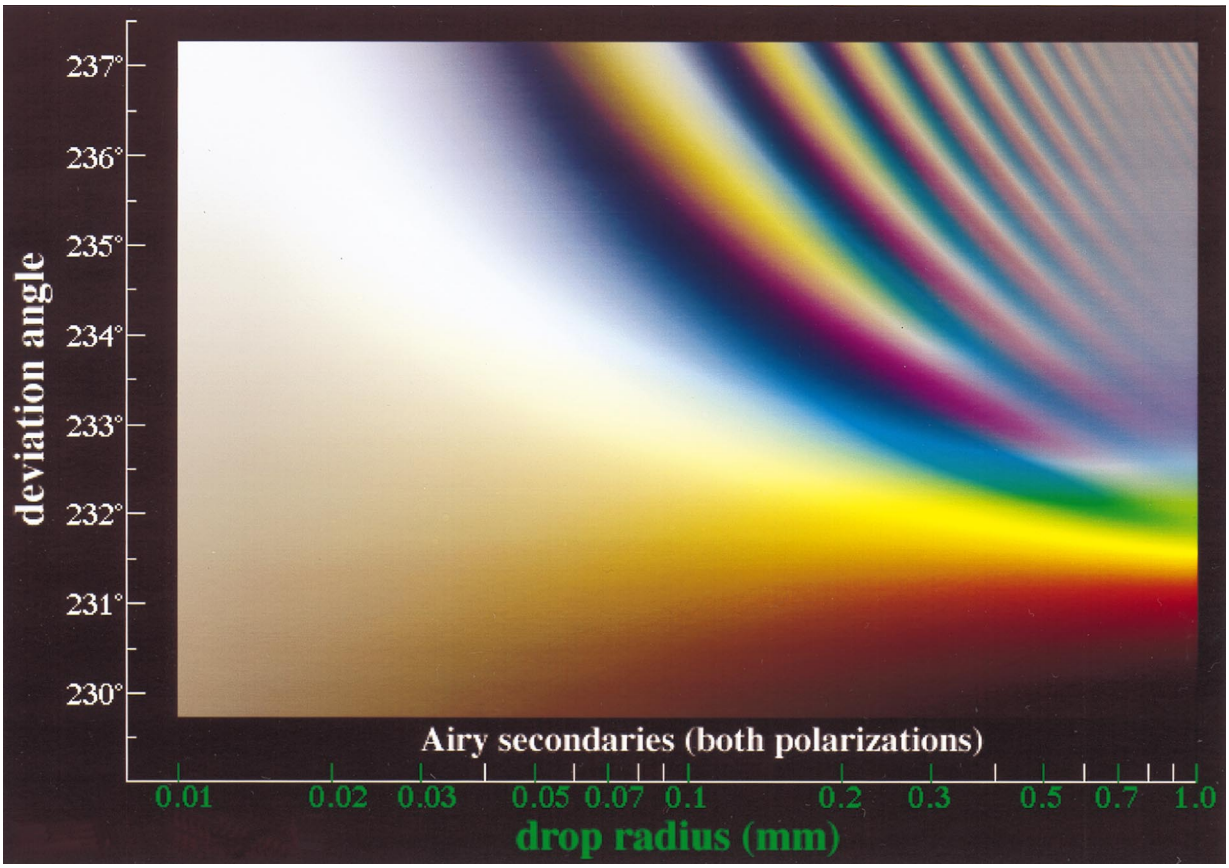

Fig. 16. Map of Airy theory colors for monodisperse secondary rainbows and cloudbows. Figure 14's assumptions (1)–(4) also hold here. A colorimetrically calibrated version of this figure can be seen at the www address given in the acknowledgment.

gruent. This is largely due to the Airy cloudbow's shift to larger θ, which places its peak luminance ~1° closer to the antisolar point than for the Mie 10-μm cloudbow. Although this shift is obvious graphically, observing it in real cloudbows is problematic, as shown below.

Now we consider chromaticity differences between Mie and Airy theories for the same four monodisperse primaries (r = 10, 50, 150, and 500 μm). All chromaticities are calculated by summations from 380 to 700 nm in 5-nm steps.[26] Figure 8 shows a portion of the CIE 1976 uniform chromaticity scale (UCS) diagram. In it, the illuminant's color is marked with a +; two chromaticity curves trace the Mie and the Airy u', v' across θ for r = 10 μm. One measure of color difference between the two theories is the colorimetric distance $\Delta(u', v')$. At any deviation angle θ,

$$\Delta(u', v') = \{[u'(\theta)_{\mathrm{Mie}} - u'(\theta)_{\mathrm{Airy}}]^2 + [v'(\theta)_{\mathrm{Mie}} - v'(\theta)_{\mathrm{Airy}}]^2\}^{1/2}, \tag{3}$$

and the average $\overline{\Delta(u', v')}$ is calculated over the θ range being considered. In Fig. 8, $\overline{\Delta(u', v')} = 0.008$, ~75% greater than the mean MacAdam JND[27] of 0.004478 in the UCS region spanned by the Mie and the Airy primaries. Like the contrast tick mark used in Figs. 4–7, the MacAdam JND drawn in Fig. 8 serves as a graphical ruler of threshold difference. Thus for a 10-μm-radius drop, Mie and Airy theories produce nearly achromatic primaries that are colorimetrically distinguishable, at least on their exteriors. Figure 9's close-up view of Fig. 8 shows the differences between Mie theory's chromaticity loops and the simpler hook-shaped curve of Airy theory. Figure 10 joins Fig. 7's luminances and Fig. 9's chromaticities to give a perspective view of their combined variation. Certainly the Mie loops are physically justifiable, yet their complexity seems at odds with the simple color transitions seen in real cloudbows.[28]

Similar loops or wiggles appear on the exterior of Fig. 11's Mie chromaticity curve for a 50-μm cloud drop. However, here the wiggles are much less prominent. In fact, now the Mie and Airy chromaticities correspond much better, as is evident both graphically and numerically [$\overline{\Delta(u', v')} = 0.00571$]. Only occasionally do the two theories disagree by more than 1 JND. Figure 12 shows that at 150 μm, $\overline{\Delta(u', v')}$ has increased to 0.01037, contrary to the conventional wisdom that differences between Airy and Mie theory must always decrease with increasing drop size.[29] Another plausible assumption upset by Fig. 12 is that rainbow luminance and chromaticity extremes necessarily coincide. The Airy primary and first supernumerary (i.e., the two leftmost maxima in Fig. 5) are indicated by small

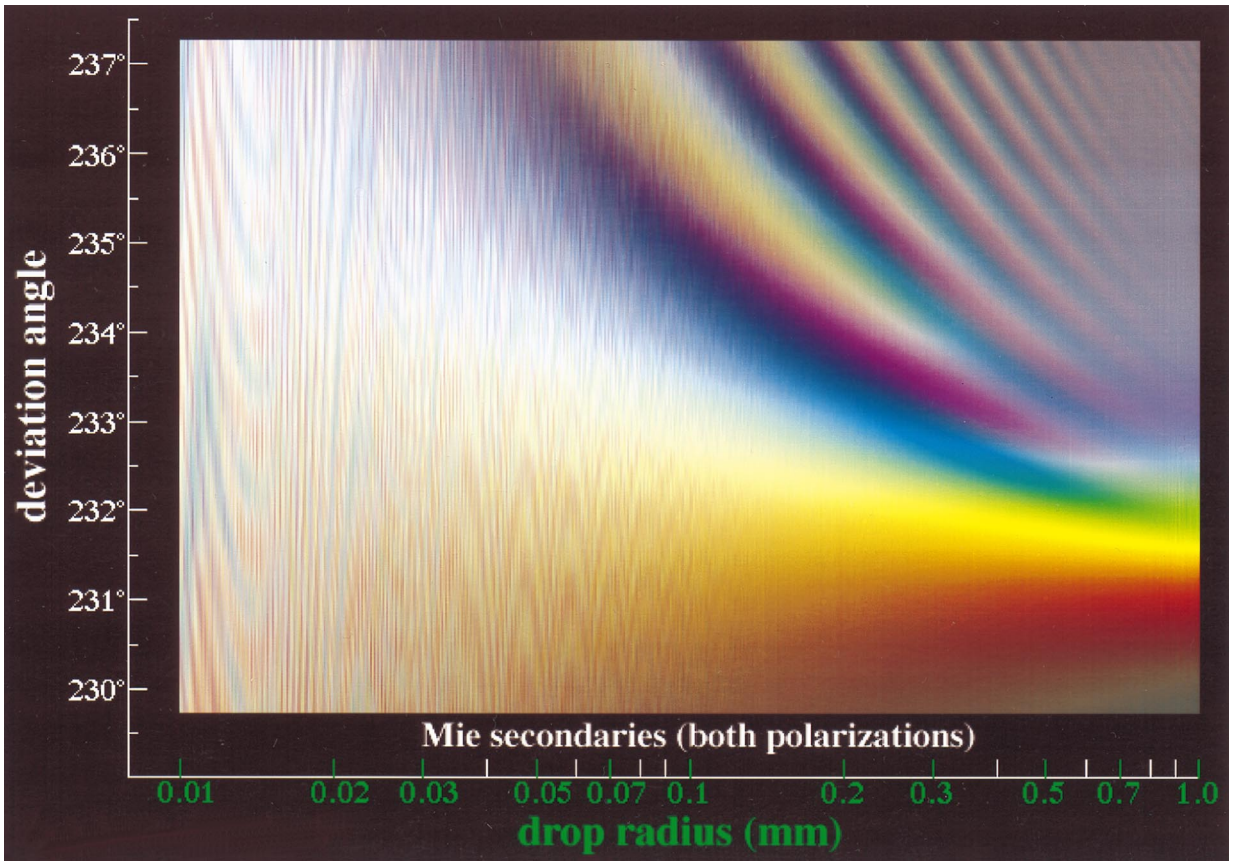

Fig. 17. Map of Mie theory colors for monodisperse secondary rainbows and cloudbows. Figure 14's assumptions (1)–(4) also hold here. A colorimetrically calibrated version of this figure can be seen at the www address given in the acknowledgment.

breaks in Fig. 12's chromaticity curve. Clearly these two luminance maxima do not have purer colors than their neighbors. In fact, Airy theory predicts that the primary's purest colors will be very dark reds on its exterior. Mie theory makes these colors both slightly brighter (see Fig. 5) and less pure than those slightly closer to the primary maximum.

The divergence between Mie and Airy colors outside the primary is even greater at a 500-μm radius (Fig. 13), and it accounts for most of the $\overline{\Delta(u', v')}$ reported there (0.01280). In fact, eliminating the smallest deviation angles ($\theta < 137.95°$) from $\overline{\Delta(u', v')}$ reduces it threefold to 0.00373. Although the Mie theory desaturation outside Fig. 13's primary is quite dramatic, we are unlikely to see it in nature, as rainbow light will be additively mixed with background light. Because luminance on the Mie 500-μm primary's exterior is ~63 times less than at its peak (Fig. 4), background light from clouds will almost always dominate colors outside the natural bow. Finally, note that the purity of Fig. 13's Airy primary has increased dramatically from that of Fig. 12. Although the dominant wavelength is ~566 nm for both, the Airy 500-μm primary is both yellower (82.3% versus 34.7% purity) and brighter than its 150-μm counterpart.

4. Color Maps of Mie and Airy Primaries

As useful as Figs. 4–13 are in plotting selected differences between the Mie and the Airy primaries, they do not convey any overall visual sense of these predicted rainbows. Because our benchmark here is the two theories' perceptual disagreement, we also need a purely visual comparison. Figures 14 and 15 provide it in the form of color maps of the Airy and Mie primaries, respectively; Figs. 16 and 17 map the Airy and Mie secondaries. The droplet radius increases logarithmically along each map's abscissa, whereas the deviation angle varies linearly along the ordinate. All maps are arranged so that their top-to-bottom color sequence is the same as that seen at the summit of the natural primary or secondary.

To make each map, standard projective geometry techniques are used to convert rainbow chromaticities to their red–green–blue equivalents on a computer's calibrated color monitor.[30] Figures 14–17 are mapped so that their white corresponds to Fig. 3's achromatic u', v'. (Your achromatic u', v' depends on the illuminant with which you view Figs. 14–17.) Neither a computer monitor nor the printed page can adequately reproduce colors throughout the luminance dynamic range shown in Figs. 4–7. Thus each column of monodisperse colors in Figs. 14–17 is normalized by the maximum luminance found at that

drop size. In other words, Figs. 14–17 do not show the enormous range of rainbow luminances evident in Figs. 4–7. Like Figs. 4–13, Figs. 14–17 assume (1) Fig. 3's solar spectrum as the illuminant, (2) Eq. (2)'s sun-width smoothing filter, (3) both rainbow polarizations, (4) spherical, nonabsorbing water drops, and (5) monodisperse colors. A monodisperse comparison is, of course, far stricter than that possible in the natural bow.

The most striking feature of Figs. 14 and 15 is their essential similarity. Even at cloud-drop sizes, the positions of the Airy and the Mie primary maxima *appear* nearly identical (but see Fig. 7). In fact, the only literally unnatural feature seems to be the Mie map's ripple structure, which appears as a subtle color marbling on the cloudbow primaries and their supernumeraries. As drop radius increases, in both Figs. 14 and 15 the primary and the supernumeraries converge into ever-narrower bands. At drop radii >0.4 mm, Mie and Airy supernumeraries are nearly achromatic and individual supernumeraries are often blurred because of Eq. (2)'s smoothing. At those same sizes, we can also see that Alexander's dark band is brighter for Mie than Airy theory (see Fig. 4).

Quantitatively, a pixel-by-pixel comparison of Figs. 14 and 15 shows that only 5.32% of all Mie and Airy rainbow colors have $\Delta(u', v') > 0.02$.[31] Color distances >0.02 are largely confined to Alexander's dark band at large drop sizes, where very low luminances render these large mismatches essentially meaningless. For pixels with $\Delta(u', v') \leq 0.02$, $\overline{\Delta(u', v')} = 0.005885$, and its standard deviation = 0.003873. Thus the average Mie–Airy color distance only slightly exceeds the primary rainbow JND. In fact, over 41% of all Airy colors here are within one JND of their Mie counterparts (i.e., compare Airy and Mie colors at the same θ and r). For the difficult conditions of outdoor color matching, even 2 JND's are a defensible threshold, in which case over 79% of Airy theory colors would be confused with their Mie counterparts. Any presumed colorimetric chasm between the two theories now looks considerably smaller. In fact, much of the Airy–Mie $\Delta(u', v')$ is due to the Mie ripple structure, which is not seen in natural bows.

A similar comparison of luminance contrast in Figs. 14 and 15 yields a mean C_v of -0.02267 with a standard deviation of 0.1141. For a threshold contrast $|C_v| = 0.02$, some 31% of the two maps' pixels would be confused. Furthermore, the positions of primary and supernumerary luminance peaks and valleys in Figs. 14 and 15 are quite close at most drop sizes. This means that subthreshold contrasts occur at all drop sizes, not just at raindrop sizes. Quantitatively, monodisperse Airy primaries often do depart perceptibly from their Mie counterparts. Yet qualitatively, these Airy primaries look more natural than do the Mie rainbows and cloudbows. By this I mean that each monodisperse Airy rainbow more closely resembles a naturally occurring polydisperse rainbow or cloudbow than does its Mie counterpart.

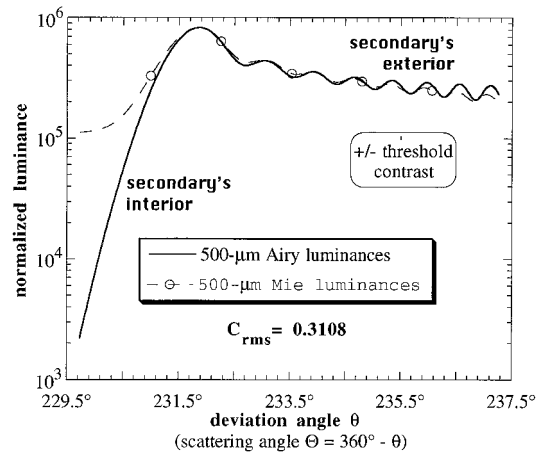

Fig. 18. Normalized Mie and Airy theory secondary luminances as functions of deviation angle θ for a single 500-μm-radius raindrop (both polarizations). The illuminant is Fig. 3's sunlight spectrum.

5. Monodisperse Comparisons of Mie and Airy Secondaries

Mie and Airy secondaries might be expected to differ more than the primaries, and Figs. 18–21 do indeed show greater luminance differences in the secondaries. Aside from a different range of θ, all other Mie and Airy theory conditions are unchanged from those of Figs. 4–7.[32] In the secondary, note that scattering angle $\Theta = 360° - \theta$ and that θ itself is now located $\theta - 180°$ from the antisolar point. In Fig. 18, C_{rms} has more than doubled to 0.3108 from Fig. 4's value, with most of the increase due to Airy underestimates of luminances in Alexander's dark band ($\theta < 231°$). Similar contrast increases are evident in Figs. 19–21, where C_{rms} ranges from 0.2839 to 0.2946. As these figures' tick marks indicate, contrast between the monodisperse Mie and Airy secondaries usually exceeds threshold. Next we examine the angular shifts of Airy maxima and minima in Figs. 19–21

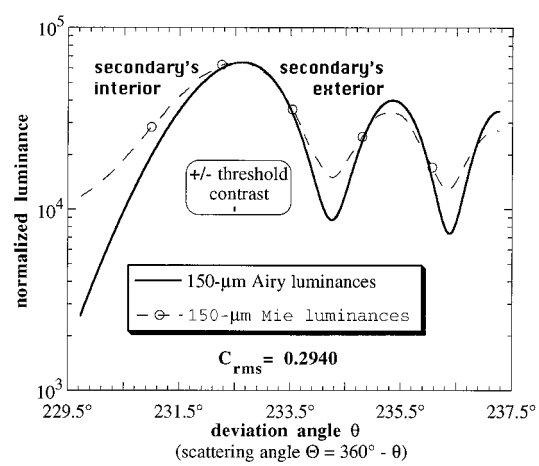

Fig. 19. Normalized Mie and Airy theory secondary luminances as functions of deviation angle θ for a single 150-μm-radius drizzle drop (both polarizations).

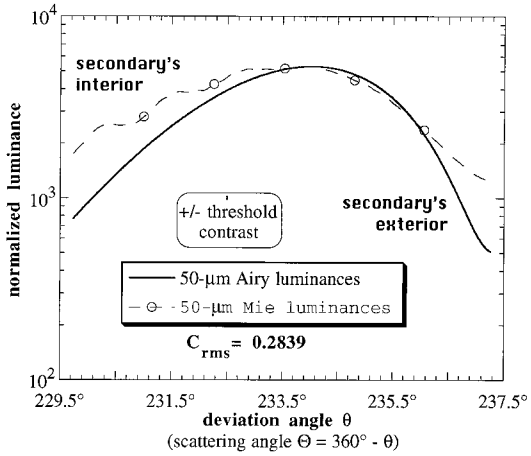

Fig. 20. Normalized Mie and Airy theory secondary luminances as functions of deviation angle θ for a single 50-μm-radius cloud drop (both polarizations).

from the Mie positions. These shifts are larger than similar Airy displacements in the primaries (Figs. 5–7).

Comparing Figs. 4 and 18, note that the Mie:Airy luminance ratio in Alexander's dark band is much larger in the secondary than in the primary. The same is true at other drop sizes, meaning that Airy theory consistently makes this part of the secondary too dark. Similarly, the Mie:Airy luminance ratio is slightly larger for supernumerary minima in Fig. 19 than in Fig. 5. (Also note that the Airy supernumerary maxima are too bright in Fig. 19.) Mathematically, this occurs because the Airy secondaries' ⊥- and ‖-polarized intensities remain in phase, unlike their primary counterparts.[33] In other words, Airy theory's ‖-polarized component increases minima *less* in its secondaries than in its primaries, where the ‖- and the ⊥-polarized components are almost completely out of phase. Thus a deficiency of the Airy ‖-polarized primary (its out-

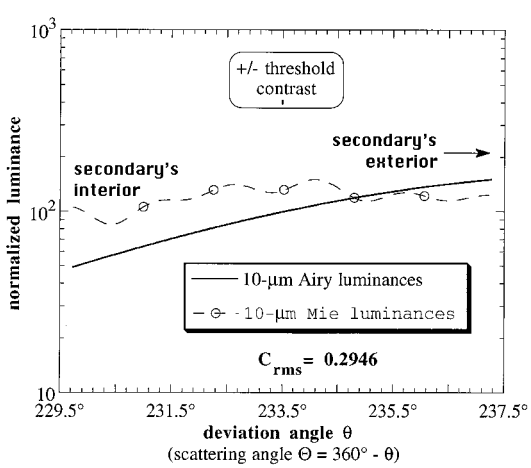

Fig. 21. Normalized Mie and Airy theory secondary luminances as functions of deviation angle θ for a single 10-μm-radius cloud drop (both polarizations).

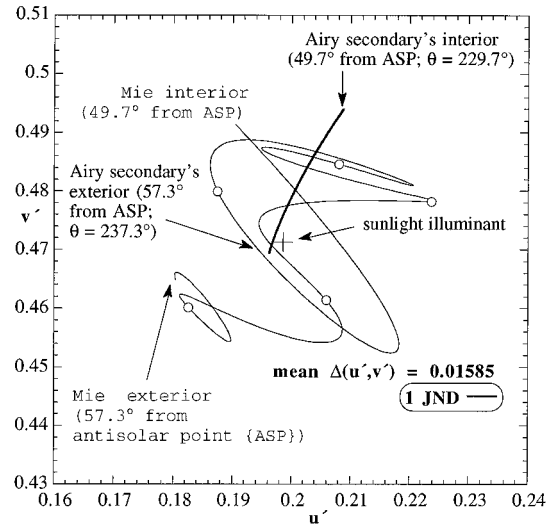

Fig. 22. Chromaticity curves for the 10-μm-radius Airy and Mie theory secondaries differ by $\overline{\Delta(u', v')} = 0.01585$ (both polarizations). The mean MacAdam JND in the u', v' region spanned by the Mie and the Airy secondaries =0.004773.

of-phase behavior)[34] actually improves the Airy primary's fit to Mie theory at some drop sizes, provided that we consider both polarizations (e.g., Fig. 5).

The Mie and the Airy secondary chromaticities also yield some counterintuitive results. These are shown in Figs. 22–25, where $\overline{\Delta(u', v')}$ consistently increases with drop size. The secondaries' $\overline{\Delta(u', v')}$ are much larger than the primaries', being some 3 to 8 times greater than the mean MacAdam JND of 0.004773 for Mie and Airy secondaries. Yet despite the mathematical and physical rigor that underlies the Mie chromaticity curves, they appear quite literally unnatural. In Fig. 22, the 10-μm-radius Mie chromaticities trace out a convoluted curve that differs starkly from the simple arc of the Airy secondary

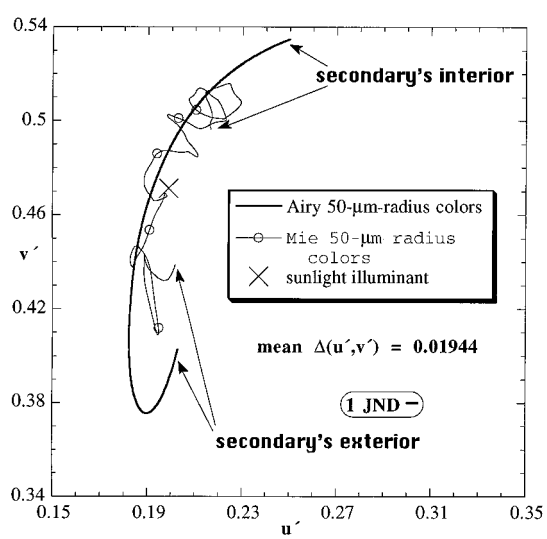

Fig. 23. Chromaticity curves for the 50-μm-radius Airy and Mie theory secondaries differ by $\overline{\Delta(u', v')} = 0.01944$ (both polarizations).

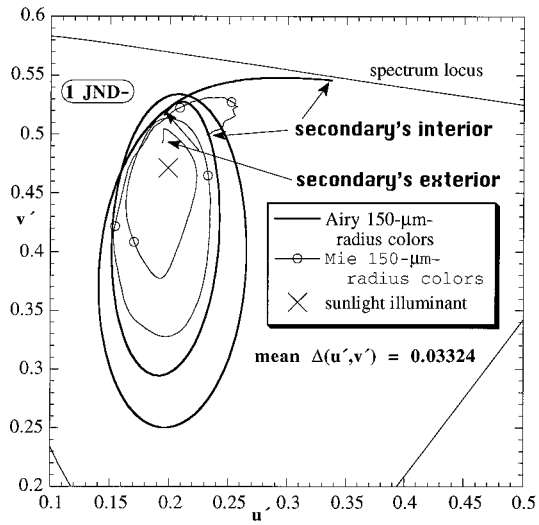

Fig. 24. Chromaticity curves for the 150-μm-radius Airy and Mie theory secondaries differ by $\overline{\Delta(u', v')} = 0.03324$ (both polarizations).

cloudbow. Of course, at this drop size not all the secondary is visible for $229.7° < \theta < 237.3°$, but the difference between the two theories is clear enough.

At 50-μm-radius (Fig. 23), the Airy colors resemble a curved frame for the irregular helix of Mie chromaticities. Near the center of the Airy curve, color distances are subthreshold more often than at 10 μm, yet the 50-μm $\overline{\Delta(u', v')}$ is greater because Airy theory predicts a larger color gamut (i.e., the Airy curve extends beyond the Mie curve).[35] For a 150-μm-radius drizzle drop, Fig. 24's Mie and Airy chromaticities at first look similar to their Fig. 12 counterparts. However, $\overline{\Delta(u', v')}$ is 3 times larger in Fig. 24, a consequence of the Mie secondary tracing a tortuous path within its smaller gamut. In fact, these Mie wiggles are colorimetric manifestations of Fig. 17's skewed color bands at 150 μm, themselves a result of the color ripple structure. At 500-μm radius (Fig. 25), the Mie secondary chromaticities ripple only occasionally, and like Fig. 13's Mie primaries, they rapidly desaturate within Alexander's dark band. Although Fig. 25's Mie and Airy curves are hardly congruent, their similar shapes seem as noteworthy as their large $\overline{\Delta(u', v')}$.

Given the secondaries' dramatically larger $\overline{\Delta(u', v')}$, Figs. 16 and 17 are surprising. Although these color maps do differ, they are not the distant relatives that Figs. 18–25 suggest. Beginning at $r \sim 0.07$ mm in Fig. 16, Airy theory's underestimates of minimum supernumerary luminances are evident (i.e., corresponding luminance minima are darker than in Fig. 17). Also evident is the consistently brighter Alexander's dark band in Fig. 17's lower right-hand corner. Colorimetrically, 12.1% of Fig. 16's Airy pixels are within 1 JND of corresponding Mie pixels in Fig. 17; 32.4% are within 2 JND's. As in the primary, many of the largest Airy colorimetric errors in the secondary occur at low luminances in Alexander's dark band, where they are unlikely to be visible. Similarly, significant numbers of subthreshold $\Delta(u', v')$ and C_v are found at all drop sizes in Fig. 16, although they do occur more frequently at larger sizes.

Although we know objectively that some Airy supernumeraries are shifted (e.g., Figs. 20–21), gross discrepancies are difficult to see in Fig. 16. In part this is due to the distracting color marbling of Fig. 17's Mie ripple structure below $r \sim 0.1$ mm. [Note that the disappearance of this structure at larger radii is just an artifact of Fig. 17's (and Fig. 15's) angular resolution.] In fact, Fig. 17's color marbling nearly obscures the smaller drops' subtle luminance peaks. At drizzle and raindrop sizes ($r > 0.1$ mm), the two maps show that Mie and Airy secondaries are almost indistinguishable visually. Furthermore, despite its larger quantitative errors, Fig. 16's Airy

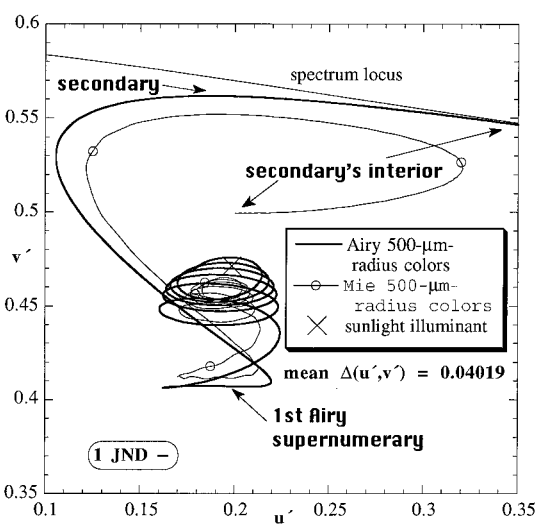

Fig. 25. Chromaticity curves for the 500-μm-radius Airy and Mie theory secondaries differ by $\overline{\Delta(u', v')} = 0.04019$ (both polarizations).

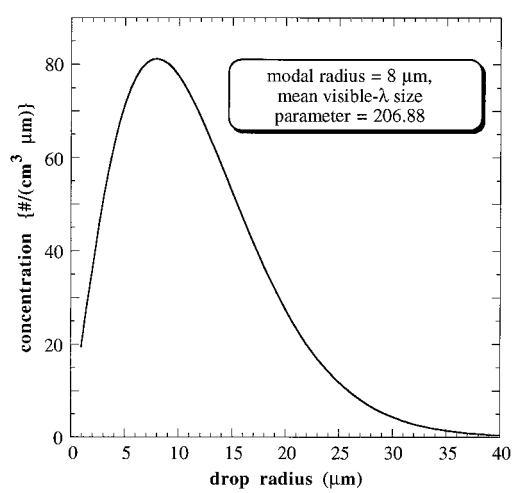

Fig. 26. Deirmendjian modified gamma distribution for drop sizes typical of stratocumulus or fog, 1–40-μm radii. This polydispersion produces the smoothed Mie and Airy theory data shown in Figs. 27–30.

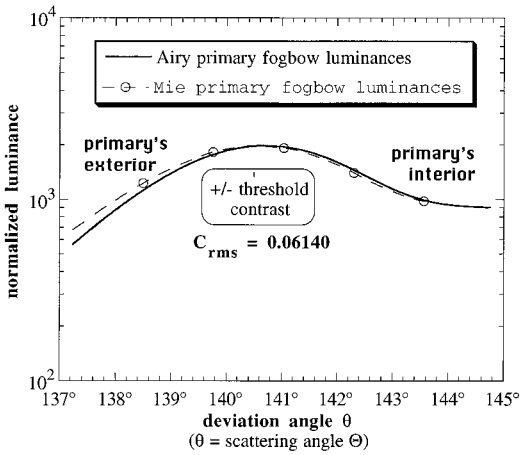

Fig. 27. Normalized luminances for Mie and Airy primary fogbows as functions of deviation angle θ for Fig. 26's drop-size distribution (both polarizations). In this and subsequent figures, the illuminant is Fig. 3's sunlight spectrum.

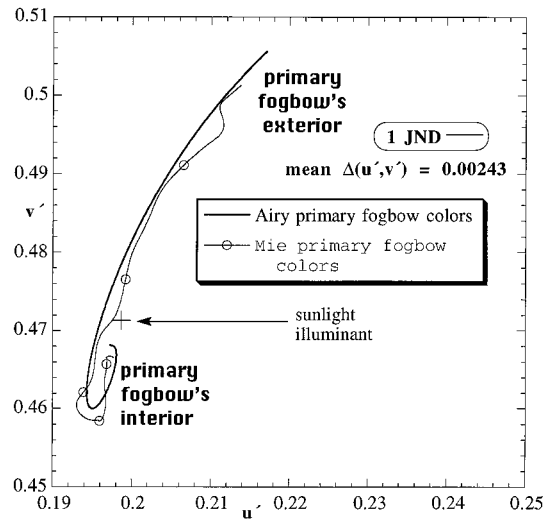

Fig. 29. Chromaticity curves for the Airy and the Mie primary fogbows differ by $\overline{\Delta(u', v')} = 0.00243$ (both polarizations).

map arguably offers a clearer picture of natural secondary bows than does Fig. 17.[36] Like its primary counterpart (Fig. 14), Fig. 16 seems the more useful qualitative guide to rainbows and cloudbows viewed with the naked eye.

6. Toward Real Fogbows: Mie and Airy Polydispersions

As instructive as Figs. 4–25 are, they still lack an important natural detail—smoothing over a realistic drop-size spectrum. Because Airy theory supposedly differs most from Mie theory at small drop radii, I integrate over a polydispersion of cloud droplets. Here I use a Deirmendjian modified gamma distribution that is representative of drop-size spectra observed in stratocumulus and fog (Fig. 26).[37] Not surprisingly, when Mie and Airy luminances are weighted by Fig. 26's droplet number densities, the resulting primary and secondary fogbows resemble each other more closely than do the monodisperse 10-μm-radius bows shown above. In Fig. 27, C_{rms} for the primary Mie and Airy fogbows has been reduced 43% from its Fig. 7 value. Figure 28's secondary fogbows show smaller improvement; there C_{rms} has dropped ~9% compared with that of Fig. 21. Luminance ripples have vanished from Fig. 27's Mie primary and are all but absent in Fig. 28's secondary.[38]

Mie–Airy colorimetric distances are affected even more than luminances by a fog polydispersion. Figure 29's primary fogbow $\overline{\Delta(u', v')}$ of 0.00243 is nearly 70% smaller than that in Fig. 9 (10-μm primary), and Fig. 30's secondary fogbow $\overline{\Delta(u', v')}$ of 0.0071 is 55% smaller than that in Fig. 22 (10-μm secondary). The Airy primary is now within 1 JND of its Mie equivalent, and the Airy secondary probably would be indistinguishable as well. Figure 29 also reveals how the Mie color ripple structure disappears in the pri-

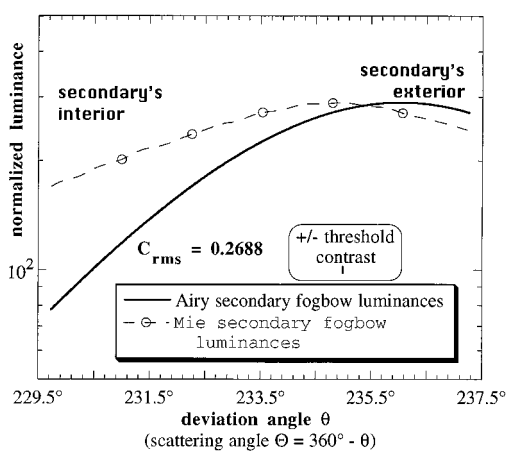

Fig. 28. Normalized luminances for Mie and Airy secondary fogbows as functions of deviation angle θ for Fig. 26's drop-size distribution (both polarizations).

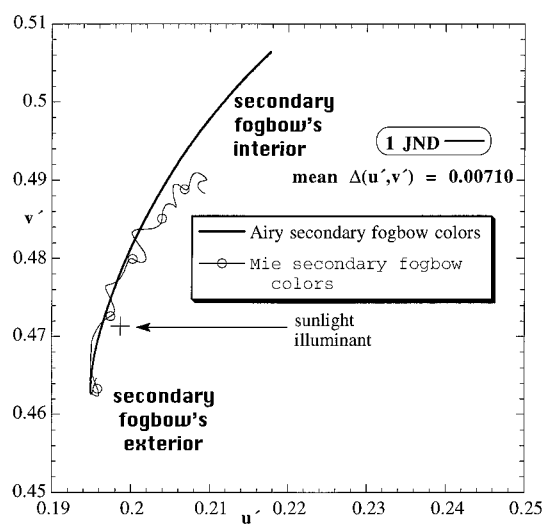

Fig. 30. Chromaticity curves for the Airy and the Mie secondary fogbows differ by $\overline{\Delta(u', v')} = 0.00710$ (both polarizations).

Table 1. Summary of Chromaticity Distances $\overline{\Delta(u', v')}$ and mean contrast C_{rms} between Mie and Airy Theory Rainbows and Cloudbows[a]

Drop Radii (μm)	Primary C_{rms} (⊥ and ‖)	Primary $\overline{\Delta(u', v')}$ (⊥ and ‖)	Secondary C_{rms} (⊥ and ‖)	Secondary $\overline{\Delta(u', v')}$ (⊥ and ‖)
10	*0.1082*	0.0080	0.2946	*0.01585*
50	0.1240	*0.00571*	*0.2839*	0.01944
150	0.1122	0.01037	0.2940	0.03324
500	**0.1327**	**0.01280**	**0.3108**	**0.04019**
10–1000 monodisperse	$\overline{C_v} = -0.0227$	0.005885	$\overline{C_v} = -0.1421$	0.01034
1–40 fogbow	0.06140	0.00243	0.2688	0.00710

[a]The first four rows are based on Figs. 4–13 and 18–25, and for these comparisons, minima are in *italic* type and maxima are in **boldface** type. Entries in the row labeled 10–1000-μm monodisperse are averages over Figs. 14–17. The last row's entries refer to Figs. 27–30.

mary fogbow: the Mie chromaticity curve straightens out along the Airy arc. In Fig. 30, the secondary's greater width makes it easier to see more angular detail, thus making the Mie curve's chromaticity wiggles more obvious there. However, compared with the two theories' stark colorimetric differences in Fig. 22, they agree much more closely in Fig. 30. Thus even at the most demanding (i.e., smallest) droplet sizes, smoothing over a natural polydispersion largely eliminates perceptible differences between the Mie and the Airy theory bows. Furthermore, my own digital image analyses of natural cloudbows reveal smooth luminance and chromaticity curves more akin to Airy than Mie theory.[35,39]

7. Conclusions

Table 1 summarizes the color and luminance differences between Mie and Airy theory discussed above. One of its most remarkable features is that, for single drops, Airy's largest color and contrast errors occur at the biggest radii (500 μm here). However, if we interpret errors as angular displacements of primaries, secondaries, and supernumeraries from their Mie theory positions, then Airy theory errors do indeed increase with decreasing drop size. For both primaries and secondaries, many of the largest Mie–Airy $\Delta(u', v')$ occur in Alexander's dark band, where low luminance usually renders them invisible. Although color differences are often subthreshold, contrasts are not, and these are largest for the Airy secondaries. In addition, angular shifts from the positions of Mie maxima and minima are larger in the Airy secondaries than in the primaries.

However, from a purely *visual* standpoint, the Airy monodisperse bows (Figs. 14 and 16) look more naturalistic[40] than their Mie kin (Figs. 15 and 17), and they do so because they lack some of the latter's spectral detail. Furthermore, if we include a polydispersion in our calculations (Figs. 27–30), Airy and Mie theories become perceptually indistinguishable even at cloud-drop sizes. Thus, far from being an outdated irrelevancy, Airy theory shows itself to be a simple, quantitatively reliable model of the natural rainbow's colors and luminances. Provided that we restrict ourselves to spectrally integrated luminances (or radiances), it can be used to predict accurately the visual appearance of most naturally occurring waterdrop bows and supernumeraries. Equally important, we see that Mie theory for monodispersions should not always be the model of first resort, as it produces details not seen in the natural rainbow and does so with much more computational effort than Airy theory.

This research was supported by U.S. National Science Foundation grant ATM-9414290. Additional funding came from the Commander, Naval Meteorology and Oceanography Command. I am indebted to Günther Können for providing me with an extension of his earlier work on polarized Airy theory.

Colorimetrically calibrated versions of Figs. 14–17 can be viewed at http://www.nadn.navy.mil/Oceanography/papers/RLee_papers.html. This address is case sensitive. If this link is outdated, write to the author by post or email (raylee@nadn.navy.mil) for the figures' current location.

References and Notes

1. G. B. Airy, "On the intensity of light in the neighbourhood of a caustic," Trans. Cambridge Philos. Soc. **6,** 379–403 (1838). Airy read his paper before the Society in May 1836 and March 1838. Remarkably (at least from the biased standpoint of atmospheric optics), Airy makes no mention of this signal accomplishment in his *Autobiography* (Cambridge U. Press, Cambridge, 1896). Instead, Airy's memorable events from 1836–1838 include his improved filing system for Greenwich Observatory's astronomical papers!
2. C. B. Boyer, *The Rainbow: From Myth to Mathematics* (Princeton U. Press, Princeton, N.J., 1987; reprint of 1959 Thomas Yoseloff edition), pp. 304–310.
3. Ref. 2, p. 313.
4. For a notable exception, see K. Sassen, "Angular scattering and rainbow formation in pendant drops," J. Opt. Soc. Am. **69,** 1083–1089 (1979).
5. G. Mie, "Beiträge zur Optik trüber Medien, speziell kolloidaler Metallösungen," Ann. Phys. **25,** 377–445 (1908). An English translation is available as G. Mie, "Contributions to the optics of turbid media, particularly of colloidal metal solutions," Royal Aircraft Establishment library translation 1873. (Her Majesty's Stationery Office, London, 1976).
6. H. M. Nussenzveig, "The theory of the rainbow," in *Atmospheric Phenomena* (Freeman, San Francisco, 1980), pp. 60–71.
7. Reference 6's arguments appear in greater detail in H. M. Nussenzveig, "Complex angular momentum theory of the rainbow and the glory," J. Opt. Soc. Am. **69,** 1068–1079 (1979).
8. Perpendicular (⊥) and parallel (‖) directions here are measured with respect to the scattering plane defined by Sun, water drop, and observer. This plane's orientation changes around the rainbow arc.
9. H. C. van de Hulst, *Light Scattering by Small Particles* (Dover, New York, 1981; reprint of 1957 Wiley edition), p. 247.
10. S. D. Mobbs, "Theory of the rainbow," J. Opt. Soc. Am. **69,** 1089–1092 (1979).
11. G. P. Können and J. H. de Boer, "Polarized rainbow," Appl. Opt. **18,** 1961–1965 (1979).
12. Ref. 6, p. 70.

13. R. T. Wang and H. C. van de Hulst, "Rainbows: Mie computations and the Airy approximation," Appl. Opt. **30,** 106–117 (1991).
14. W. J. Humphreys, *Physics of the Air* (Dover, New York, 1964; reprint of 1940 McGraw-Hill edition), pp. 491–494.
15. R. A. R. Tricker, *Introduction to Meteorological Optics* (American Elsevier, New York, 1970), pp. 179–181.
16. Ref. 11, p. 1963.
17. C. F. Bohren and D. R. Huffman, *Absorption and Scattering of Light by Small Particles* (Wiley, New York, 1983), pp. 112–113, 477–481.
18. Ref. 7, p. 1073 (Fig. 3). Note that Fig. 1's Mie curve includes small-scale structure due to external reflections, whereas Nussenzveig's figure does not.
19. Ref. 17, pp. 300–304.
20. Exceptions include bows seen from mountains, hills, and airplanes in flight.
21. The effects of this smoothing on rainbow luminance are also shown in A. B. Fraser, "Chasing rainbows: numerous supernumeraries are super," Weatherwise **36,** 280–289 (1983).
22. Rather than combine color and luminance differences in a single color-difference measure, I show them separately here. Although rainbow observers cannot make this separation, it does let me address more readily the issues raised in Refs. 6, 7, 9, and 13. Optically speaking, cloudbows and fogbows differ very little, so the terms can be used interchangeably.
23. See Ref. 9, p. 247.
24. J. Gorraiz, H. Horvath, and G. Raimann, "Influence of small color differences on the contrast threshold: its application to atmospheric visibility," Appl. Opt. **25,** 2537–2545 (1986).
25. Similar Airy underestimates of intensities in Alexander's dark band are evident in Ref. 7, p. 1073 (Fig. 3).
26. G. Wyszecki and W. S. Stiles, *Color Science: Concepts and Methods, Quantitative Data and Formulae*, 2nd ed. (Wiley, New York, 1982), pp. 158–164.
27. Ref. 26, pp. 306–309.
28. D. K. Lynch and W. Livingston, *Color and Light in Nature* (Cambridge U. Press, Cambridge, 1995), p. 119 (Fig. 4.10A). Also see R. A. Anthes, J. J. Cahir, A. B. Fraser, and H. A. Panofsky, *The Atmosphere*, 3rd ed. (Merrill, Columbus, Ohio, 1981), Plate 19b, opposite p. 468.
29. Eliminating deviation angles outside the primary where the Mie and the Airy 150-μm chromaticities diverge noticeably ($\theta < 137.8°$) reduces $\overline{\Delta(u', v')}$ to only 0.008901. That still exceeds the 50-μm cloud drop's $\overline{\Delta(u', v')}$ of 0.00571.
30. Reference 26, pp. 138–139. Similar techniques are used in R. J. Kubesh, "Computer display of chromaticity coordinates with the rainbow as an example," Am. J. Phys. **60,** 919–923 (1992). Figures 14–17 each contain more than 219,000 pixels.
31. All chromaticity and luminance differences are calculated with the real-number data that underlie Figs. 14–17.
32. In a personal communication, G. P. Können (Royal Netherlands Meteorological Institute, De Bilt, The Netherlands) kindly extended Ref. 11's mathematics to include both polarizations of the Airy secondary.
33. Können and de Boer clearly show this phase relationship (Ref. 11, p. 1964).
34. Ref. 6, p. 70.
35. R. L. Lee, Jr., "What are 'all the colors of the rainbow'?," Appl. Opt. **30,** 3401–3407, 3545 (1991).
36. In fact, secondary supernumeraries are seen only rarely in nature. See G. P. Können, "Appearance of supernumeraries of the secondary rainbow in rain showers," J. Opt. Soc. Am. A **4,** 810–816 (1987).
37. E. J. McCartney, *Optics of the Atmosphere: Scattering by Molecules and Particles* (Wiley, New York, 1976), pp. 163, 170 (Figs. 3.19 and 3.22).
38. Although Nussenzveig notes in passing that monodisperse ripples will be averaged out "over a range of size parameters," he does not dwell on the point (Ref. 7, p. 1079).
39. R. L. Lee, Jr. and A. B. Fraser, *The Rainbow Bridge: Rainbows in Art, Myth, and Science* (Penn State Press, University Park, Pa., to be published), Figs. 8-22 and 8-23.
40. Consistent with my definition of the natural rainbow, naturalistic here means "as seen in naturally occurring polydisperse bows."